Synoptic-Dynamic Climatology of the "Bomb"

FREDERICK SANDERS AND JOHN R. GYAKUM

Department of Meteorology, Massachusetts Institute of Technology, Cambridge 02139

(Manuscript received 24 March 1980, in final form 12 June 1980)

ABSTRACT

By defining a "bomb" as an extratropical surface cyclone whose central pressure fall averages at least 1 mb h^{-1} for 24 h, we have studied this explosive cyclogenesis in the Northern Hemisphere during the period September 1976–May 1979. This predominantly maritime, cold-season event is usually found ~400 n mi downstream from a mobile 500 mb trough, within or poleward of the maximum westerlies, and within or ahead of the planetary-scale troughs.

A more detailed examination of bombs (using a 12 h development criterion) was performed during the 1978–79 season. A survey of sea surface temperatures (SST's) in and around the cyclone center indicates explosive development occurs over a wide range of SST's, but, preferentially, near the strongest gradients. A quasi-geostrophic diagnosis of a composite incipient bomb indicates instantaneous pressure falls far short of observed rates. A test of current National Meteorological Center models shows these products also fall far short in attempting to capture observed rapid deepening.

1. Introduction

Tor Bergeron is reputed to have characterized a rapidly deepening extratropical low as one in which the central pressure at sea level falls at the rate of at least 1 mb h^{-1} for 24 h. An extreme example of the development of a storm of this type appears in Fig. 1. The extraordinary deepening occurred during an interval of unfortunately sparse coverage of ship observations near the center, so that we know the central intensity only at the initial and final times. Note that nearly the strongest winds occur only ~60 n mi from the center, and that the radial profile of wind near the center must resemble that of a tropical cyclone. Note further that the storm develops along the leading edge of an outbreak of bitterly cold air over the western Atlantic, but that the cold air does not penetrate to the center of the low.

A Defense Meteorological Satellite view (Fig. 2), about midway through the illustrated period, shows a major "head cloud" mass of great meridional extent, considered by Jalu (1973) and by Böttger *et al.* (1975) to be characteristic of intense deepening on a small scale. Note also the indication of deep convection along the rear edge of the main cloud mass, corresponding to the cold front, and the eyelike circular clear area perhaps 40 n mi in diameter near 43°N, 43°W, near the estimated position of the surface center. These characteristics also appear to be typical.

We are interested in this phenomenon because of its great practical importance to shipping and to coastal regions. Even pleasure craft are endangered by these storms; the tragic loss of life in the 1979 Fastnet yacht race was attributable to a rare summer example of the meteorological "bomb" (Rice, 1979). We are also interested in these storms because (as will be shown later) deepening rates predicted by current operational dynamical models fall far short of the observed ones, implying that some physical effect other than the commonly understood large-scale baroclinic mechanism may play an important role. Finally, the rapid deepening process may be a necessary component in a realistic model simulation of the general circulation. We have tested the notion that most of the hemisphere's deepest cyclones (which usually track toward their final resting places in the vicinity of the Icelandic and Aleutian lows) have deepened explosively. Of the 37 deep lows (960 mb or lower) found during the 9-month period beginning 1 September 1978, 31 qualified as a bomb (using the criteria defined in Section 4) during their development. Thus, explosive deepening is a characteristic of the vast majority of the deepest cyclones.

2. A three-year data sample

For three recent cold seasons we have studied this class of explosively intensifying cyclones in the Northern Hemisphere from longitude 130°E eastward to 10°E. As Bergeron's characterization probably referred to the latitude of Bergen (60°N), a geostrophically equivalent rate was obtained for arbitrary latitude ϕ by multiplying his rate by

0027-0644/80/101589-18$08.50

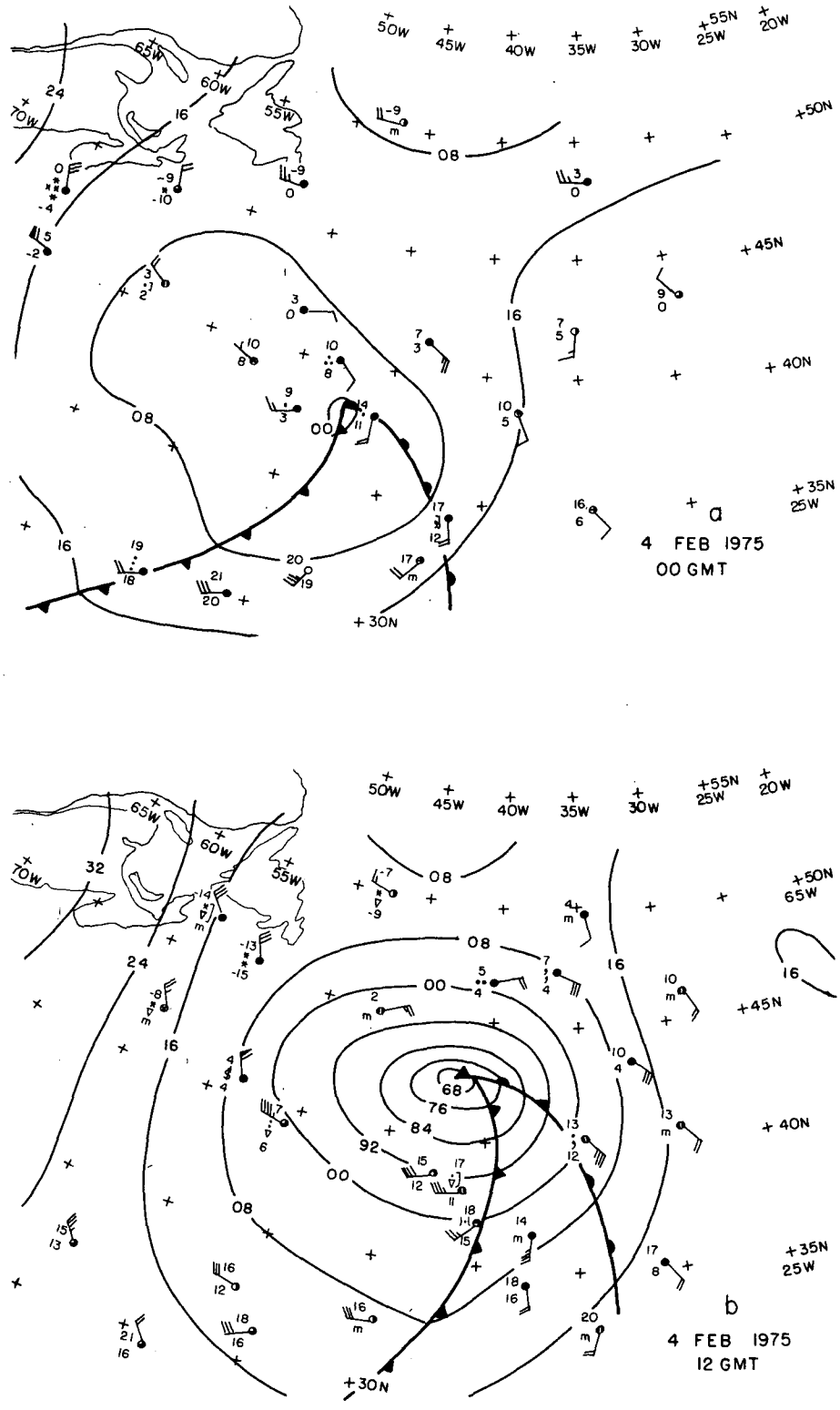

FIG. 1. Surface maps, with isobars of sea level pressure at 8 mb intervals. Selected ship observations are represented by a simplified plotting model. Pressures, not shown, agree closely with isobars. Six-hour positions along the track of the center are shown as dots along the dashed trajectory.

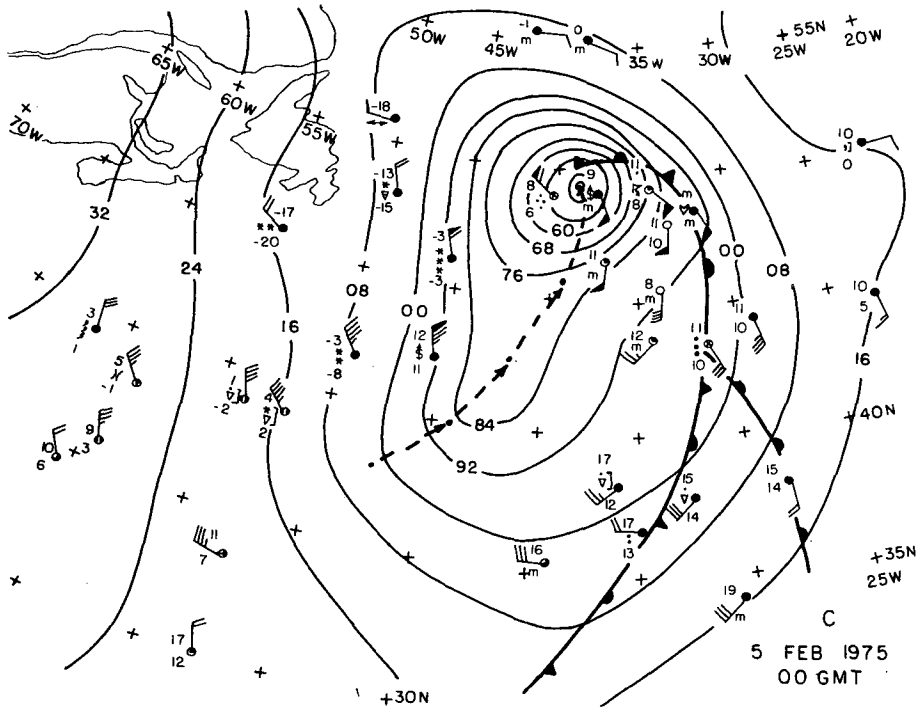

FIG. 1. (*Continued*)

($\sin\phi/\sin 60$). The resulting critical rate, which we denote as 1 bergeron, varies from 28 mb (24 h)$^{-1}$ at the pole to 12 mb (24 h)$^{-1}$ at latitude 25°N, the southern limit of the phenomenon in our sample.

Fig. 3 displays the 0000 GMT locations of 267 bombs during the periods 2 October 1976–30 March 1977, 10 September 1977–31 March 1978 and 9 September 1978–13 April 1979. The raw deepening was obtained, with few exceptions, by comparing the 1200 GMT central pressures of a low on successive days as shown in the analysis prepared by the National Meteorological Center (NMC) and received on the National Facsimile Circuit.

It is clear that the bomb is primarily a maritime event, with appreciable overland frequencies only over the eastern United States. Pronounced frequency maxima occur in the westernmost portions of both the Atlantic and Pacific Oceans, 5–10° of latitude poleward of the zone of maximum winter initial cyclogenesis frequency shown by Petterssen (1956, p. 267) and within or just north of the warm waters of the Gulf Stream and the Kuroshio, respectively.

In the Pacific there appears to be an additional center of comparable strength between longitudes 160 and 170°W, where Petterssen's (1956, p. 267) map shows a minor maximum of cyclogenesis frequency and where other sources (e.g., Haurwitz and Austin, 1944) show a mean winter position of a polar front distinct from the one in the western part of the ocean.

In the Atlantic there are extensions of modest bomb frequency north of latitude 50°N east of Labrador and in an extended region from the western approaches to Ireland and the United Kingdom to the Barents Sea. There is a notable lack of explosive cyclogenesis in the Aleutians and in the Greenland-Iceland area, where mean

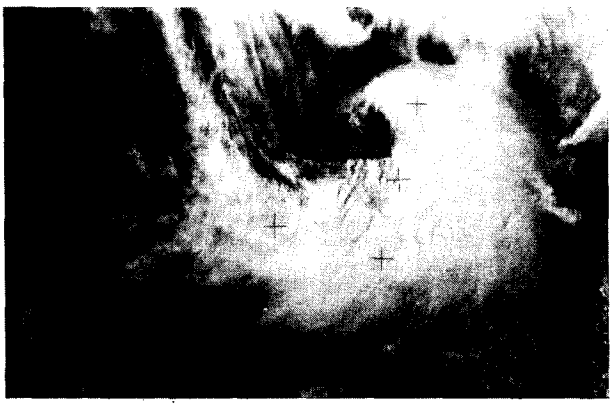

FIG. 2. Visible DMSP view of the storm at 1345 GMT 4 February. Three colinear cross-hairs represent locations, from top to bottom, 45°N, 45°W; 45°N, 40°W and 45°N, 35°W. The remaining two represent similarly, locations 40°N, 45°W and 40°N, 35°W.

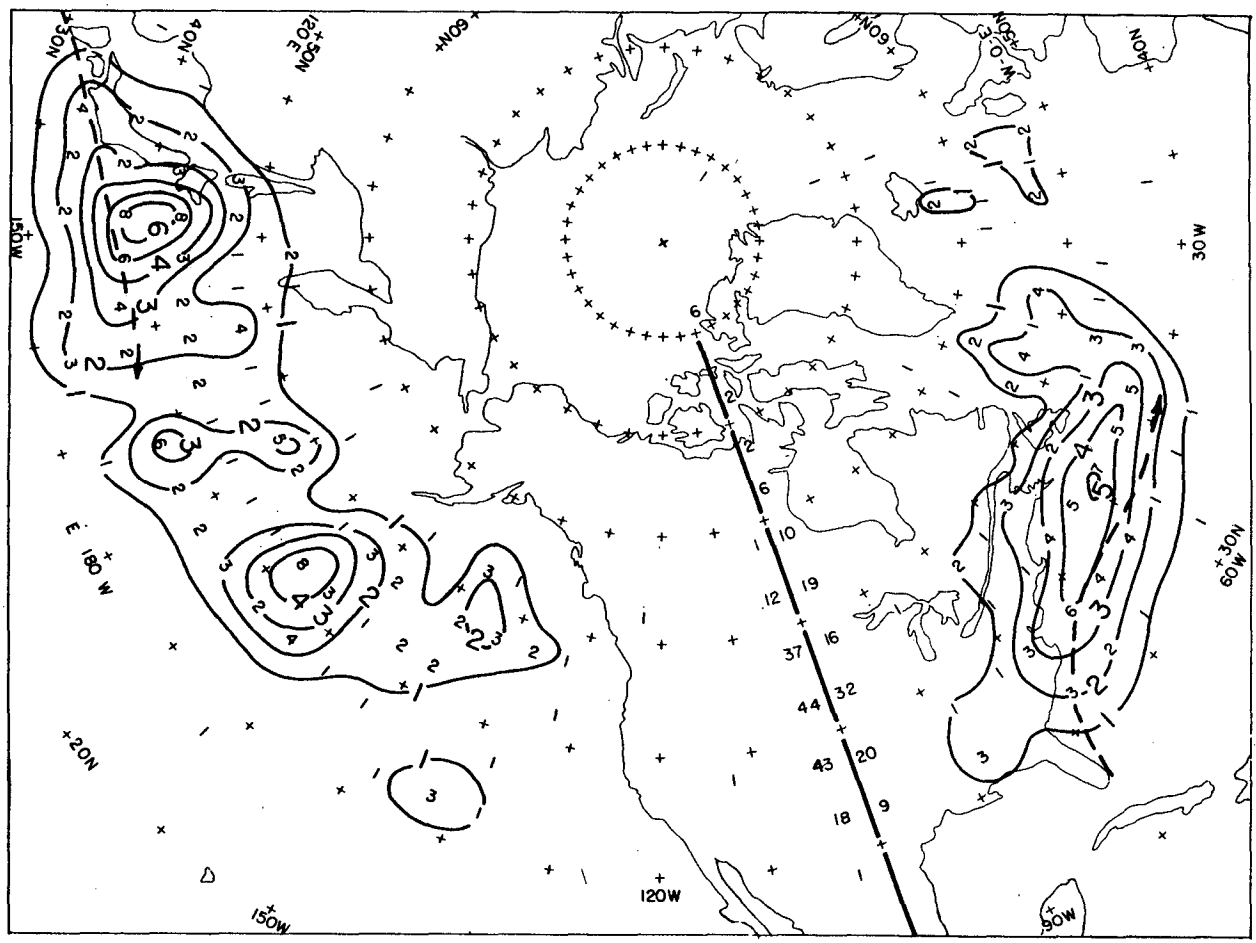

FIG. 3. Distribution of bomb events during three cold seasons. Raw non-zero frequencies appear in each 5° × 5° quadrilateral of latitude and longitude. Isopleths represent smoothed frequencies, obtained as one-eighth of the sum of four times the raw central frequency plus the sum of the surrounding raw frequencies. The column of numbers to the left and right of the heavy line along longitude 90°W represent, respectively, the normalized frequencies for each 5° latitude belt in the Pacific and Atlantic regions, using a normalization factor of ($\cos 42.5/\cos\phi$). Heavy dashed lines represent the mean winter position of the Kuroshio and the Gulf Stream.

winter pressure is lowest and cyclone frequency is largest. These data confirm the prevailing view that these regions are the resting places of migratory cyclones rather than sites of active cyclogenesis.

Our area of study excludes most of Europe, North Africa and Asia, where the explosively deepening cyclone is probably either absent altogether or rare, even over the Mediterranean Sea. Our period of study excludes May–August and most of April, but probably not many bombs, as can be seen in the monthly march of mean daily frequency (Fig. 4). The event is quite rare in September, peaks in January when two bombs occur each three days, then drops rapidly to half as often in March.

Our restriction to examination of only the period beginning and ending at 1200 GMT, rather than other 24 h periods, doubtless allowed some events to pass unnoticed, as the time of rapid deepening of a given cyclone is often this duration or less. We undoubtedly missed a few because of occasional loss of the facsimile maps. It is also virtually certain that some bombs escaped detection in the NMC analyses, owing to lack of a key ship observation at a key time and place. The analyses are bound to err on the side of conservatism concerning small intense vortices in regions of sparse data coverage.

In a few instances we reanalyzed a case on the basis of additional observations, resulting invariably in a greater deepening than shown in the operational analysis. The extreme value (2.8 bergerons) in Fig. 5 represents our reanalysis of the extraordinary Atlantic storm of 10 September 1978 (the seasonally earliest in our sample), in which the dragger *Captain Cosmo* was lost and the liner *Queen Elizabeth II* was damaged (NOAA, 1979). Our reanalysis shows a central pressure of 955 mb at 1200 GMT, with a 24 h deepening of 50 mb, whereas the NMC analysis showed a value of 980 mb, owing to lack of information from the liner and of the real-time observations from the freighter *Euroliner,* defining the great

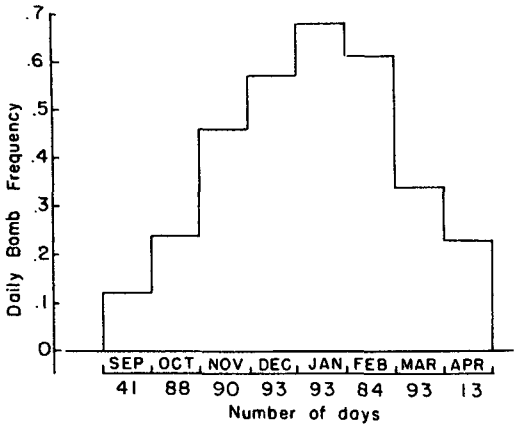

FIG. 4. Mean daily bomb frequency as a function of calendar month, for three cold seasons. The abscissa indicates the number of days considered for each.

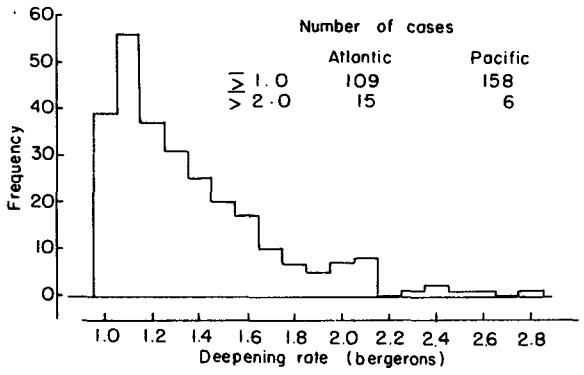

FIG. 5. Bomb frequency as a function of deepening rate, for three cold seasons.

intensity of the center. Further, the storm illustrated in Fig. 1 would have yielded an off-scale value of 3.4 bergerons had it been included in our period of study. Even given the two ship observations closely bracketing the center in Fig. 1c, we cannot determine the central pressure with great certainty. Our extrapolation of external gradient gives a central value of 935 mb. An excessively conservative estimate based on inviscid cyclostrophic flow, and on the reported pressure of 950 mb and wind speed of 50 kt at 50 n mi from the center, with tangential speed varying as the square root of central distance, yields a central value of 942 mb. These are both lower than the NMC analyzed value of 944 mb. Finally, note in Fig. 5 that although the bomb frequency is about half again larger in the Pacific than in the Atlantic, more than twice as many extreme events (≥2.0 bergerons) occurred in the latter region. This result is probably due in part to a greater density of ship observations in the Atlantic, although we will show later some evidence of its physical reality.

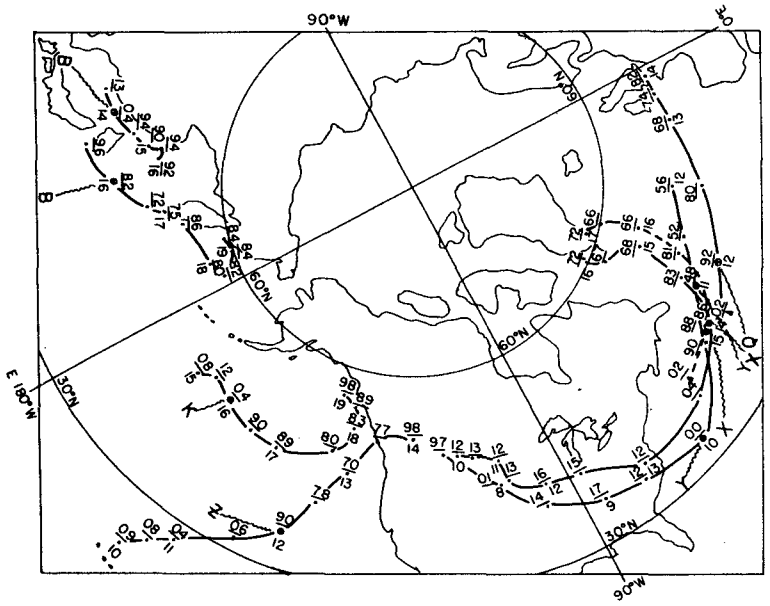

FIG. 6. Twelve-hour tracks of surface lows which produced bomb events during the period 10–16 February 1979. The date is given beneath each 00 GMT position, and the central sea-level pressure (in tens and units of millibars) is given, underlined above each position dot. The position of the bomb event is an encircled dot connected by a wriggly line to the associated, lettered mobile trough at 500 mb. The bombs in the Atlantic on the 14th and 15th both occurred at 40°N, 43°W and were separated for clarity. A triangle in place of a dot indicates a suspected initial position within a trough but no center.

We can conclude from all this that our sample underestimates both the frequency and intensity of intense oceanic cyclogenesis. We take it as an article of faith, however, that the discrepancy is not large enough to render our results meaningless.

Our results confirm those of recent studies (e.g., Blackmon *et al.*, 1977) emphasizing the importance of transient eddy transports of heat and momentum in these cyclogenetic regions for the operation of the Northern Hemispheric winter circulation. In fact our results suggest that their actual dominance may be substantially greater than illustrated in data based on NMC coarse-mesh analyses.

3. Relationship to upper level flow

To obtain a rudimentary idea of the upper level context of these intense surface cyclogenetic events, we examined our sample in relation to the daily NMC hemispheric 0000 GMT 500 mb charts received on facsimile. Our routine departmental practice is to trace the 552 dam contour of 500 mb height, identifying and tracking the mobile troughs. During the cold season, this contour lies along or just poleward of the center of the belt of strongest flow. An example appears in Fig. 7 illustrating the exceptionally active seven days from 10 through 16 February 1979.

Fig. 6 shows the lifetime tracks of each of the lows which deepened explosively during this period. Each bomb event occurred when a mobile 500 mb trough was positioned somewhere between south and west of the surface center. In the western Pacific, the two bombs were associated with the same upper trough B. The surface centers never moved far east of their origin, while Fig. 7 shows that trough B had traveled from central Asia during the days prior to surface cyclogenesis. Subsequently, this trough passed on eastward, severing connections with the dying cyclones.

In the eastern Pacific a cyclone formed and deepened rapidly when overtaken by trough K, which lay over the Yellow Sea on 10 February and passed on eastward into North America after the 16th, while the surface cyclone lost its identity in the Gulf of Alaska. An earlier second bomb in the eastern Pacific had developed from a trough in the easterlies over the Hawaiian Islands, then moved northeastward and deepened explosively when interacting with upper trough Z approaching from the northwest. The surface cyclone filled and died on crossing the coast of British Columbia

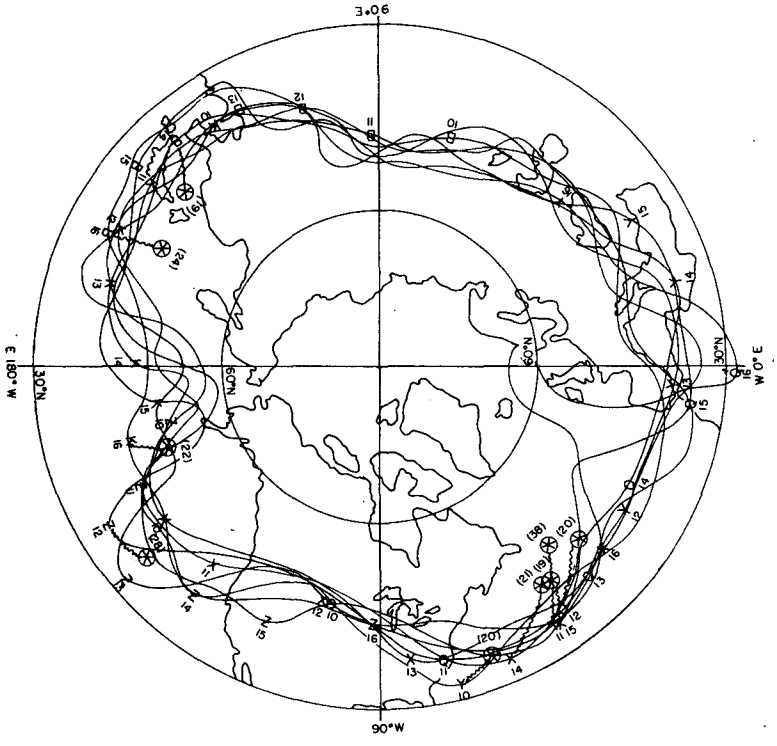

FIG. 7. Positions of the 552-dam contour of 500 mb height at 00 GMT 10–16 February 1979. Mobile 500 mb troughs associated with the surface bombs are identified by letter and date. Wriggly lines connect trough with bomb (shown as circled asterisks with 24 h pressure drop in parentheses) as in Fig. 6. Bombs in the Atlantic were separated as in Fig. 6.

while the upper trough continued eastward into the continent.

In the western Atlantic, Figs. 6 and 7 show a veritable string of explosions. Events were initiated when a low originating in the lee of the Rockies moved over the Gulf Stream in association with upper trough Y, beginning a spectacular deepening from 1012 mb at 1200 GMT 9 February to 948 mb at 0000 GMT 11 February. This system qualified as two bomb events on the 10th and 11th. (Note that had we included the 24 h period centered on 1200 GMT the 52 mb deepening centered at this time on the 10th, representing 3.2 bergerons, would have been larger than any in our sample.) This cyclone proceeded to the eastern Atlantic, filling and losing its identity, while the trough continued on to the Caucasus on the 16th.

Other Atlantic events were less dramatic. A weakly defined center, associated with wave Q, formed in the cold air southwest of the center discussed above, in the manner described by Reed (1979) for the Pacific Ocean. The fall of central pressure was not accompanied in this case, by a particularly large growth of circulation intensity. A low formed in the lee of the Rockies on the 10th, associated with upper trough X, and moved with this trough to the western Atlantic, where rapid deepening occurred on the 14th. The same upper trough was associated with rapid cold-air cyclogenesis southwest of this bomb a day later. The two resulting cyclones moved northward on remarkably similar tracks with nearly identical central pressures, the later one being slightly farther east. Both died near the southern tip of Greenland while the initiating trough X moved eastward.

It is interesting and suggestive that this cluster of Atlantic bombs was the prelude to a spectacular breakdown of the zonal flow over southern Europe, starting with wave amplification in the eastern Atlantic the last three days of this period and, during the days immediately following, culminating in a cutoff anticyclone over Scandinavia and cyclone over the Mediterranean Sea.

Students in the synoptic laboratory were asked to locate the nearest mobile 500 mb trough for each surface bomb in the months October–March. In 252 cases, excluding the few in September and April and a few more for which the interpretation was ambiguous, they found the upper trough in the surface cyclone's southwest quadrant 78%, northwest 13%, southeast 6% and northeast 2% of the instances. The mean displacement from the surface center to the trough on the 552 dam contour was toward the west-southwest at a distance of ~400 n mi. This position of the upper trough at the latitude of the maximum westerlies is qualitatively typical of deepening baroclinic cyclones. The overtaking of the deepening surface center by the mobile 500 mb trough is similar to the scenario provided by Petterssen (1956, p. 335). There are quantitative difficulties with this explanation, however, as we shall see.

A view of bomb occurrence in relation to the larger scale quasi-steady flow was obtained by reference to "envelope charts" prepared weekly in the department. The envelope chart for 10–16 February 1979 appears in Fig. 8. As can be seen by comparison with Fig. 7, this chart is prepared simply by connecting the northernmost and southernmost of the daily positions of the 552 dam contour associated, respectively, with the mobile ridges and troughs. The position of each of 256 bombs for the months October–March was placed in the appropriate envelope chart. Fig. 8 shows four bombs occurring within the envelope (hence within or just poleward of the region of maximum 500 mb wind and baroclinicity), with five occurring to the north, in the colder air. The sample of 256 includes 54% within the envelope, 38% in colder air to the north, and 7% in warmer air to the south. This circumstance points to the importance of both large-scale horizontal temperature contrasts and transfer of latent and sensible heat from the winter ocean into relatively cold air.

There is a current controversy concerning the baroclinic versus the convective nature of the relatively weak polar lows in the eastern Atlantic (Rasmussen, 1979). Rosenblum and Sanders (1974) have analyzed a similar case on the New England coast in which both aspects appear to have been present. It seems likely that our bombs represent baroclinic events, strongly (and perhaps crucially) aided by diabatic heating of a type not yet elucidated and by the relative smoothness of even a rough sea surface.

Our bomb sample can also be stratified according to longitudinal position in the envelope chart. Note the troughs in Fig. 8 near 130°E, 140°W and 65°W, with ridges near 170, 105 and 20°W. The region of southwest flow in the envelope chart was defined as extending from one-quarter to three-quarters of the way from a quasi-steady trough to the downstream ridge. The northwest flow region extends similarly from ridge to downstream trough. The remaining sectors are defined as the trough and ridge regions.

Fig. 8 depicts two western Pacific bombs—one each in trough and southwest-flow regions. In the eastern Pacific one bomb occurs in northwest flow and one in the trough region; the western Atlantic contains four in southwest flow and one in the trough region. Using the 256 cases, including many which could not be stratified so unambiguously, the laboratory students estimated 41% to be in the southwest-flow region, 37% in the trough region, and 11% each in the northwest-flow and ridge regions. Clearly, the region about one-quarter of

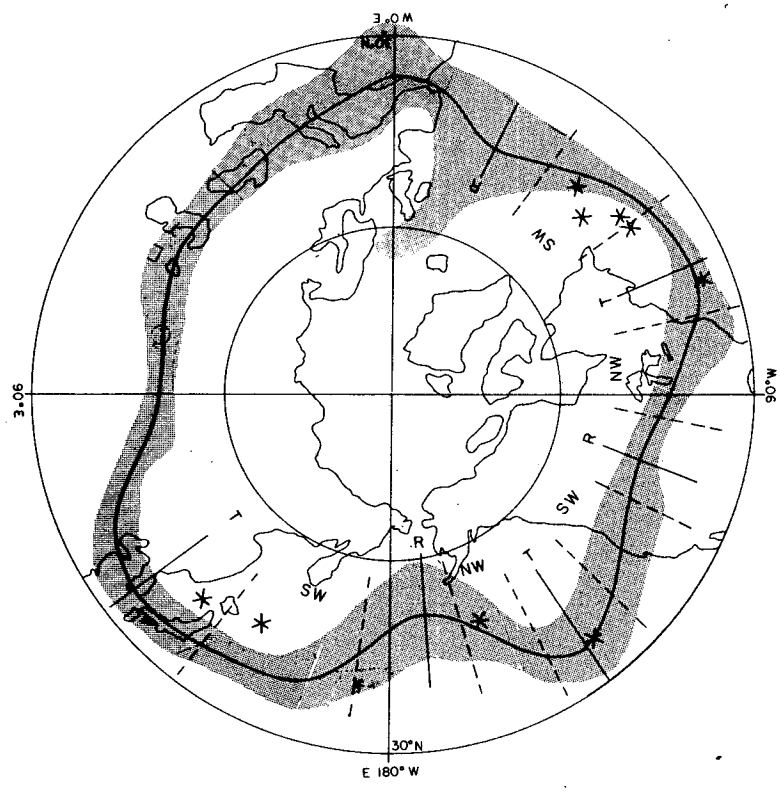

FIG. 8. Envelope chart for the period 10–16 February 1979, with bomb positions shown as asterisks. Bombs separated in the Atlantic as in Fig. 6 both lie in southwest sector.

the distance from a quasi-steady trough to the ridge is favored for explosive cyclogenesis.

These findings are consistent with the result of Frederiksen's (1979) linear stability analysis, in which regions of preferential development are favored just downstream from the planetary wave trough. Our cyclogenesis, like Fredericksen's, occurs preferentially poleward of the local maximum vertical shear. We find a strong preference for the smooth, relatively warm, maritime environment, with implied physical effects not addressed in his model.

The converse effect of cyclone-scale instability on development of larger scales has also recently received renewed theoretical attention. The increase in amplitude of the planetary waves in the eastern Atlantic and western Europe following the 10–15 February bomb cluster in the western Atlantic is an egregious local example of the type of behavior studied by Gall *et al.* (1979). It appears that interactions between relatively small intense bombs and planetary-scale troughs and ridges may work both ways.

4. A detailed study of the 1978–79 season

In order to examine more closely the physical process of explosive cyclogenesis, we made a detailed study of the period from 1 September 1978–31 August 1979. A bomb for this study is defined as one in which the deepening rate is the geostrophic equivalent of at least 12 mb in 12 h at 45°N.

Fig. 9a indicates the monthly distribution of the 150 bombs recorded during this period. As mentioned earlier, these explosive events reach a peak in the cold season, with a few isolated occurrences indicated during the summer months. Figs. 9b and 9c represent the corresponding distributions for the Atlantic (east of 80°W) and Pacific (west of 120°W) basins, respectively. Only three cases occurred outside these regions. Although Fig. 9a indicates peak frequencies in December and January, such is not the case for the individual basins. Peaks occur in December and February in the Pacific and Atlantic, respectively. February was persistently cold across the eastern United States (Dickson, 1979), especially during the extraordinarily active period 10–16 February previously discussed.

Fig. 10 represents the frequency distributions of normalized central pressure tendencies for this sample. The two Atlantic events at the extreme values of 43 and 44 mb $(12\ h)^{-1}$ represent the cases of 10 September 1978 and 10 February 1979 discussed earlier. Note that 16% of the Atlantic cases had normalized 12 h central pressure tendencies of 24 mb or more, while only ~8% of the Pacific

cases fell into this category. This is consistent with results reported earlier for the 3-year sample of 24 h bombs.

We can examine a possible time bias in the data. The 0000–1200 GMT deepeners represent 45% of the total sample, 44% of the Pacific sample and 46% of the Atlantic sample. An unbiased normal distribution of 0000–1200 GMT frequencies for the Pacific yields a 15% probability of so few 0000–1200 GMT deepeners while a similar distribution yields a corresponding probability of 26% for the Atlantic. Neither statistic gives us much confidence that a time bias exists in either basin, although uneven data coverage in time may play a role in our statistics.

The geographical distribution of 1978–79 12 h bombs is indicated in Fig. 11. The major features of this distribution are similar to those found for the three-year sample. The primary Pacific maximum south of 40°N at about 150°E exists in both Figs. 11b and 3, with the doublet of secondary maxima between 40 and 50°N, and 170 and 160°W and in the Gulf of Alaska appearing less intense than in Fig. 3. The Atlantic basin chart indicates virtually all of the explosive cyclogenesis occurs between 40 and 75°W. Figs. 11a and 3 both reveal the sharp cutoff of bomb frequency east of 40°W.

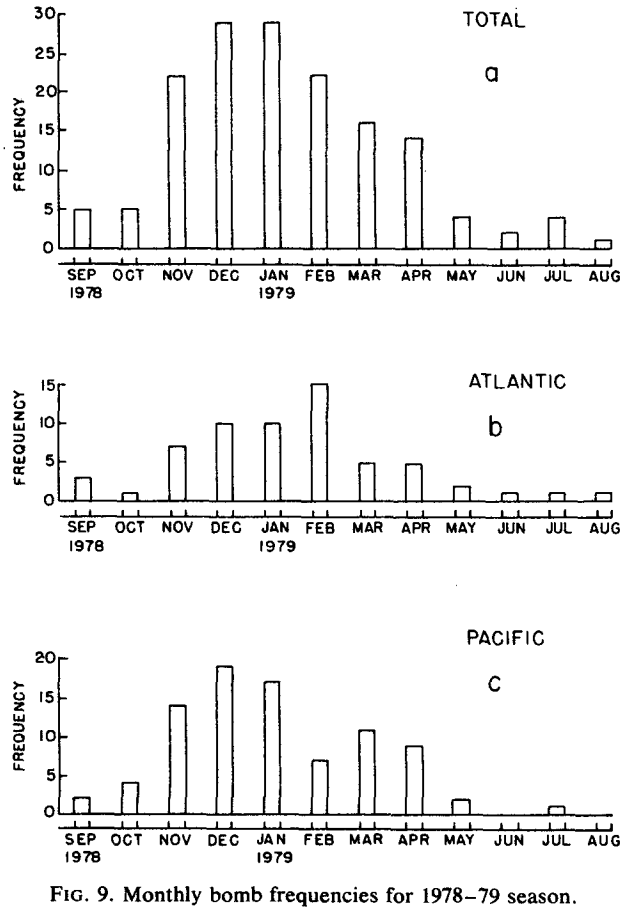

FIG. 9. Monthly bomb frequencies for 1978–79 season.

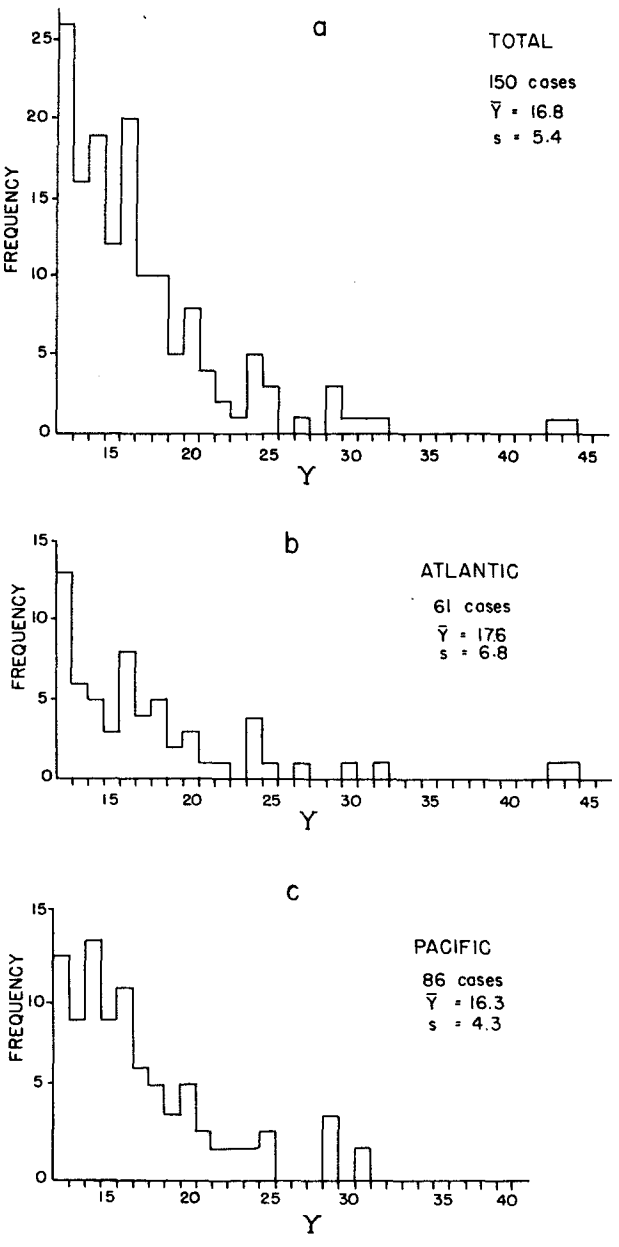

FIG. 10. Bomb frequencies as a function of normalized 12 h deepening rate Y for 1978–79. Y is 12 h central pressure fall (mb) times the normalization factor ($\sin 45/\sin\phi$), where ϕ represents the mean latitude of the cyclone center during its 12 h track. $\bar{Y}$ and s indicate the mean and standard deviation, respectively, of each sample.

5. Relationship to sea surface temperature

The deepening rates discussed above are comparable to those shown by Holliday and Thompson (1979) for tropical cyclones. We considered whether a minimum sea surface temperature is required for explosive extratropical cyclogenesis, as for tropical cyclone development. Sea surface temperatures (SST's) at the bomb center at the beginning of the 12 h growth period were obtained from daily charts

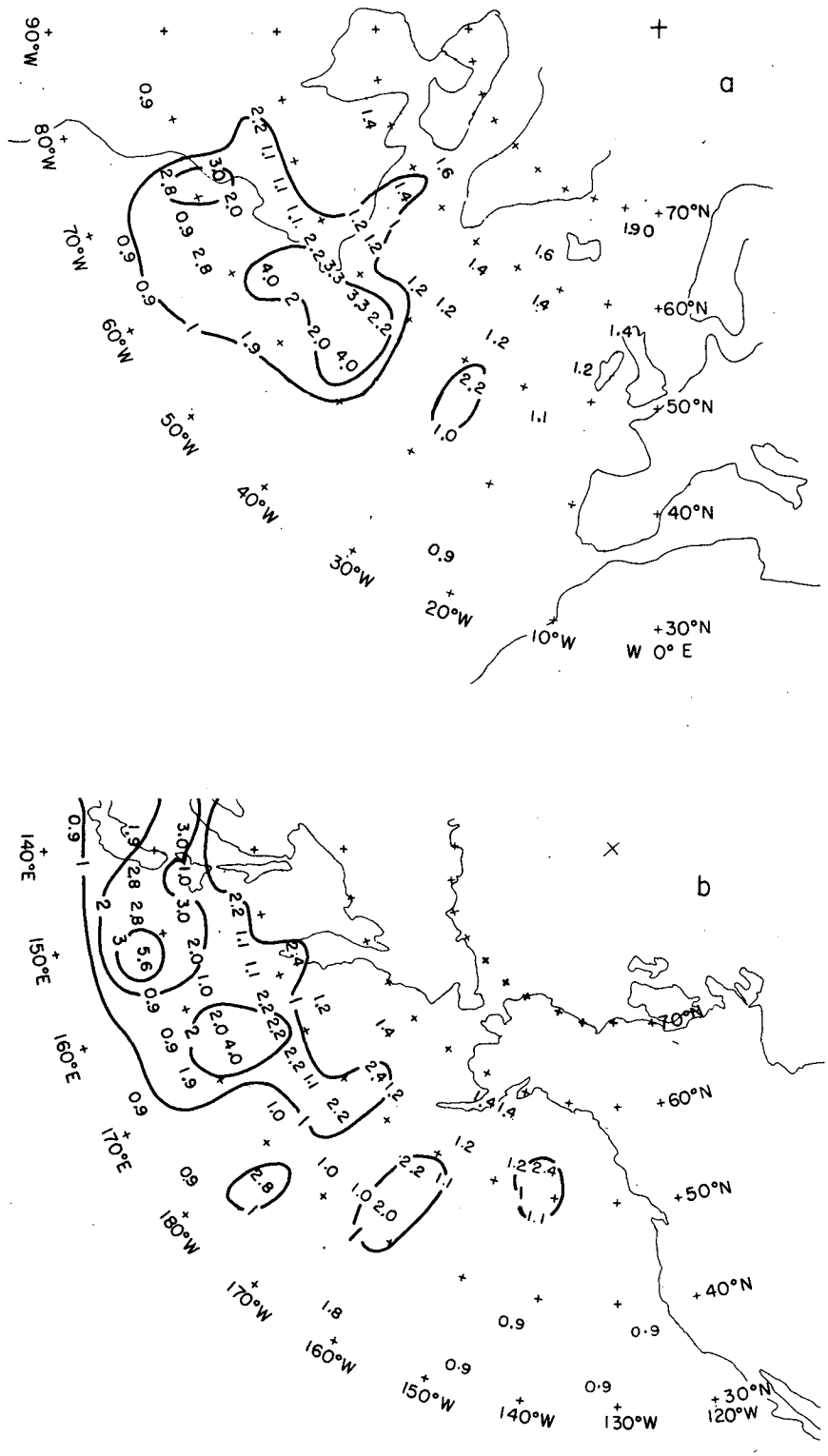

FIG. 11. Geographical distribution of bomb events for the Atlantic and Pacific basins in 1978–1979. The position of the bomb was the origin of the track segment for the qualifying 12 h period. Area-normalized non-zero frequencies appear in the appropriate 5° × 5° quadrilateral of latitude and longitude. The normalization factor is (cos42/cosϕ), where ϕ is the mean latitude for the quadrilateral.

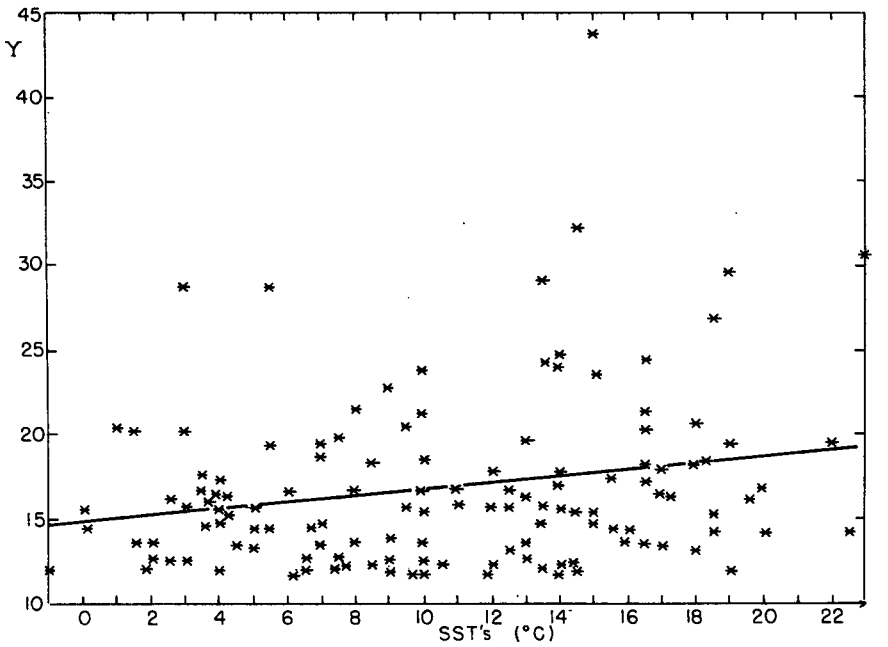

FIG. 12. A plot of all available 1978–79 bombs (indicated by asterisks) with respect to its underlying SST and its subsequent 12 h central pressure fall. The ordinate Y is defined as in Fig. 10. Solid line is the least-squares fit.

provided by the Fleet Numerical Oceanographic Center. A plot of these SST's against the normalized deepening rate appears in Fig. 12.

Bombs occur over a large range of SST's, from 0 to 23°C. When deepening was related to the warmest SST within 90 n mi of the center, results were virtually identical. There is a slight positive (0.22) correlation between the underlying SST and the 12 h deepening rate. Evidently, extratropical bombs do not display the sensitivity to SST's which tropical cyclones do, as shown observationally by Holliday and Thompson (1979) and theoretically by Miller (1958).

Nevertheless, Winston (1955) and Pyke (1965), among others, have associated rapid cyclogenesis with the strong sensible and latent heat exchange between cold continental air and the relatively warm sea surface. This exchange should be particularly intense for cold air which moves rapidly across a strong SST gradient toward relatively warm water. The resulting low static stability, in addition to low-level baroclinicity, may also play a role in rapid cyclogenesis. Staley and Gall (1977) have used a four-level quasi-geostrophic model to indicate the importance of low static stability and strong wind shear in the lower layers in enhancing growth rates of relatively short baroclinic waves. An analysis of the SST gradients would then indicate maritime areas with strong low-level baroclinicity, and with a susceptibility to a dramatic air-mass modification.

Fig. 13 shows the 15 January 1979 analyses of the magnitude of SST gradients for the Atlantic and Pacific oceans. This date was chosen because it is close to the peak period of bomb frequency. Maps for other times throughout the winter season indicate similar fields. A comparison with Fig. 11 reveals that explosive cyclogenetic events tend to occur in and around the areas of most intense SST gradients. These gradients in the Atlantic basin are strongest in longitudes west of 40°W and between latitudes 35 and 50°N, the same region where most of the Atlantic bombs occur. The gradient fields in the Pacific are more diffuse with at least 2°C differences noted throughout the band between latitudes 40 and 50°N. The maximum gradients are observed east of Japan, close to the location of the frequency maximum of Pacific bombs.

The maximum gradients in the western Atlantic are nearly twice as large as their counterparts in the western Pacific. This difference characterizes the long-term mean patterns as shown, for example, by Sverdrup *et al.* (1942, Chart II). We have noted the observed tendency for the more explosive bombs to occur preferentially in the Atlantic basin. The difference in maximum gradients suggests that this preference may be physically real, rather than an artifact of uneven data coverage.

6. Quasi-geostrophic diagnosis for 1978–79 sample

To diagnose dynamical characteristics of the storm, we have constructed composite patterns of

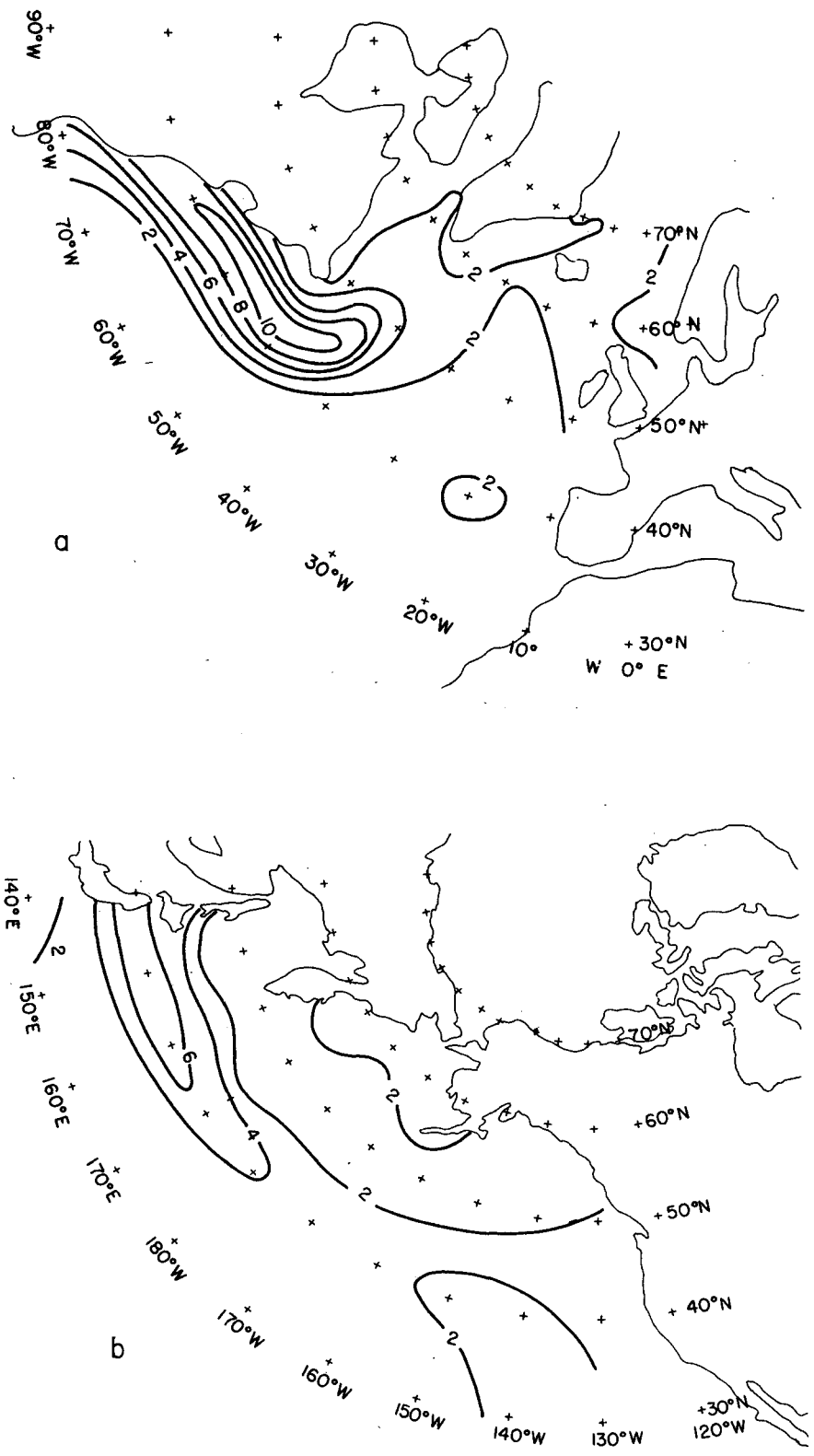

FIG. 13. Analysis of the magnitudes of the local SST gradient evaluated over a 180 nm distance interval for 15 January 1979 in the Atlantic and Pacific basins. Isopleth units are in °C (180 n mi).$^{-1}$

sea-level pressure and thickness from 1000 to 500 mb for the beginning of the 12 h period of explosive deepening. We studied disturbances originating between latitudes 40 and 50°N, a region containing 84 of the year's 150 bombs. For each case we obtained, from routine facsimile maps, three thickness lines—one for the value directly over the low center and one each for values 12 dam lower and higher. These lines were traced from 20° longitude west to 20° longitude east of the center. We also constructed two isobars representing pressures 8 and 16 mb greater than the central pressure of the low. The composite thickness patterns were obtained by averaging the patterns for the individual cases. The isobars for each case were determined by finding the radii in a polar coordinate system every 45° in direction from the low center, and composites were obtained by averaging. Because of illegible or faulty maps, missing thickness patterns, and occasional unusually distorted patterns felt to be nonrepresentative, we could use only 45 of the 84 cases in the composites. However, the frequency distribution of the normalized deepening rates in this smaller sample is quite similar to the one shown in Fig. 10. The sample was stratified on the basis of the pressure rise from the low center to the adjacent northward col. If the value was less than 16 mb the case was classified as one of weak circulation: otherwise one of strong circulation. Figs. 14a and 14b show the composites for weak and strong circulation, respectively.

The westward displacement of the thermal trough from the surface center is 600–800 n mi. This is consistent with the earlier finding of a 400 n mi west-southwestward displacement of the mobile trough in the 552 dam contour at 500 mb.

Each of the composites lend themselves readily to a diagnostic quasi-geostrophic calculation of central pressure tendency. We computed the geopotential tendencies in a quasi-geostrophic model similar to the one proposed by Sanders (1971, hereafter referred to as S). The major difference from the model in S is that we assume a horizontal temperature gradient independent of height, and a vanishing vertical motion at the 250 mb level. The expression for the geopotential tendency used for the surface center is

$$\chi_{sc} = \hat{\chi}_1\,(1000\text{ mb})\,\sin(2\pi\lambda/L). \tag{1}$$

The variable L indicates the wavelength of the tropospheric thermal trough-ridge pattern, and λ indicates the upstream displacement of the surface center from the warm ridge. Thus, $\hat{\chi}_1$ (1000 mb) is the geopotential tendency of the low center when it is located a distance $L/4$ upstream from the warm ridge. In the present model

$$\hat{\chi}_1(1000\text{ mb}) = \frac{-\eta_0 Ra\hat{T}}{(2\pi/L)T_0\gamma}\left\{\frac{[(1-2q)+q4^q-(1-q)4^{(1-q)}]k-(1-2q)\ln 4}{4^{(1-q)}-4^q}+k+1\right\}$$
$$+\frac{f_0\eta_0\hat{T}}{4(2\pi/L)^3T_0\gamma}\left(\frac{\partial f}{\partial y}\right)_0\left\{\frac{(2q-1)-q4^q+(1-q)4^{(1-q)}}{4^{(1-q)}-4^q}-1\right\}. \tag{2}$$

The analogous expression in S is Eq. (29). The variables defined above are identical to those in S. Thus η_0 is the domain-average absolute vorticity, R the gas constant, T_0 the mean tropospheric temperature (assumed a constant 250 K), and γ a dimensionless static stability parameter. A γ value of 0.063 was used in the calculations. This is based on 68 ship radiosonde observations taken at 0000 GMT in the vicinity of rapidly deepening cyclones during the period 1971–74. A saturated atmosphere is assumed in our γ value so that the temperature structure refers to the moist adiabat. The variable q is

$$q = 1/2 + 1/2(1 + 4/k)^{1/2},$$

where

$$k = \frac{f_0\eta_0}{2(2\pi/L)^2RT_0\gamma}.$$

As in S, the first term in (2) represents the active deepening mechanism for the surface center and it is due to the positive thermal vorticity advection (PTVA) over the low center. The variables a, representing the basic planetary scale temperature gradient and $\hat{T}$, indicating the perturbed part of the temperature field, are the ingredients used to estimate this PTVA. An evaluation of a and $\hat{T}$ was accomplished through a decomposition of the thickness fields in Fig. 14 into their mean and perturbed parts, using the graphical technique of Fjørtoft (1952). A 12 h central pressure fall of 3.3 mb and one of 4.0 mb were computed for the cases in Figs. 14a and 14b, respectively. This compares with the respective observed 12 h mean falls of 16.5 and 17.8 mb. These calculations were made without regard to the $\sin(2\pi\lambda/L)$ factor. The λ changes from $L/6$ in the weak circulation case to $L/7$ in the strong circulation composite. Thus, the computed pressure falls would be attenuated to 75–85% of their maximum values. In addition, the frictional filling effect was ignored. Thus, we have extracted about the maximum amount of deepening allowed by this quasi-geostrophic model.

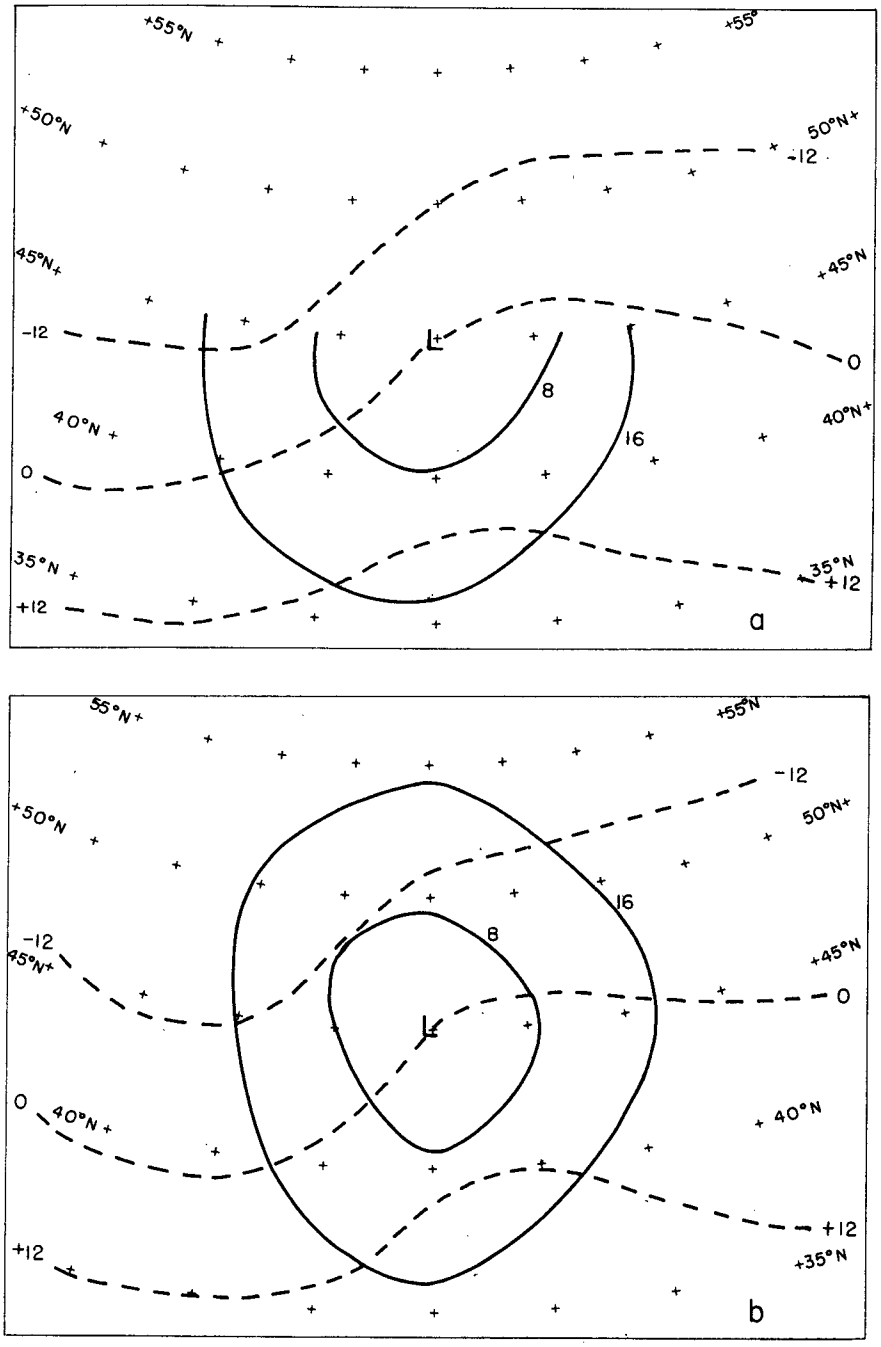

FIG. 14. Composite of the incipient bomb. Solid isopleths represent the number of millibars greater than analyzed sea-level pressure of surface center. Dashed isopleths are 1000–500 mb thickness lines (dam). (a) Weak circulation composite based on 28 cases; (b) strong circulation composite based on 17 cases.

One might question whether the averaging process destroyed much of the PTVA, since it is a nonlinear quantity, and the PTVA of the mean state is not equal to the mean of the individual values. However, an inspection of the individual cases indicates structurally similar situations, so that there does not appear to be a correlation between the basic meridional temperature gradient and the longitudinal one of sufficient magnitude to obscure the basic results of the composite. Furthermore, we have examined bomb cases individually, and have found computed central pressure falls quite similar to the above computations.

For an extreme example, a careful reanalysis of

TABLE 1. Summary of (6-L)PE and (7-L)PE model performance for observed cases of bombs. N is the number of observed bombs.

Forecast period (h)	(6-L)PE					(7-L)PE				
		Observed 12 h Δp (mb)		Model 12 h Δp (mb)			Observed 12 h Δp (mb)		Model 12 h Δp (mb)	
	N	Mean	Standard deviation	Mean	Standard deviation	N	Mean	Standard deviation	Mean	Standard deviation
12–24	46	16.3	4.7	4.7	3.8	67	16.5	5.4	6.2	5.4
24–36	45	16.4	4.7	3.8	3.8	67	16.3	5.2	4.3	5.0
36–48	43	16.7	4.8	4.0	4.1	74	16.2	5.1	5.0	5.5

the tropospheric thickness and sea level pressure fields associated with the development of the February 1975 case discussed earlier reveals corresponding diagnostic central pressure tendencies of only about 3 mb (12 h)$^{-1}$ at 0000 GMT 4 February 1975 and 9 mb (12 h)$^{-1}$ at 1200 GMT 4 February 1975. These computations compare with the observed 12 h central pressure falls of 34 mb and 30 mb. During this first 12 h period the wavelength shortened from 3400 to 2200 km and $\hat{T}$ increased from 1.0 to 2.5°C. Fig. 14b indicates the half-wavelength of the thickness pattern to be slightly shorter and better defined than in weak circulation composite although there is little difference in $\hat{T}$ of the two composites. Thus, the pattern indicated in 14b illustrates a more advanced stage in the life of the composite surface system.

Finally, Fig. 14 indicates a pattern of diffluence in the 1000–500 mb thickness fields. The thermal wind 10° longitude downstream of the surface low is no more than two-thirds the value of the corresponding thermal wind 10° longitude upstream of the surface system. Bjerknes (1954) has associated the diffluent upper level trough with developing surface cyclones, and has argued for the development of such a trough in a cyclonic-shear vorticity zone aloft. Although this forecasting rule is consistent with our earlier finding favoring development just north of the zone of maximum westerlies, and our composite indicating a pattern of diffluence in the upper level flow, a quantitative determination of surface development is still lacking.

7. Bomb prediction by NMC primitive-equation models

Although Leary (1971) has documented systematic errors in the NMC primitive-equation (PE) model (Shuman and Hovermale, 1968) predictions of surface cyclone development, a brief summary of recent NMC model performance with respect to bombs seems appropriate. The NMC PE performance was tested during the period from September 1977–May 1978, and from November 1978–March 1979. We had a unique opportunity to study the effect of horizontal resolution in the model during this period of study, for 20 January 1978 was the date NMC began operationally using the 7-layer (7-L) PE with a horizontal mesh length one-half that of the older 6-layer (6-L) PE. The horizontal grid resolution represents the essential difference between the two models, since the additional layer was added in the stratosphere.

A summary of performance of the two models for cases when 12 h bombs occurred appears in Table 1. The sample size is limited because the PE forecast domain on the facsimile maps extends westward only to the dateline, and thus excludes the major region of explosive cyclogenesis in the western Pacific. The mean non-normalized 12 h pressure fall of the observed bomb is ~16.5 mb in all cases. This sample indicates the (6-L)PE captures close to one-quarter of the observed 12 h central pressure tendency while the (7-L)PE captures about one-third of the observed tendencies. Both models dramatically underforecast this oceanic cyclogenesis. Leary (1971) also found systematic underprediction of the depth of maritime cyclones by the (6-L)PE. Druyan (1974) has found the Goddard Institute for Space Studies model (Somerville *et al.*, 1974) to be similarly deficient in forecasting deepening cyclones. Fig. 15 indicates plots of the observed versus predicted central pressure tendencies for the 12–24 h forecast category. Very few forecasts approach the observed tendencies in either model. However, the slope of the regression lines is steeper in the (7-L)PE forecasts than in the (6-L)PE predictions. The correlation coefficient for the linear regression in the (7-L)PE case is about 0.32, while the (6-L)PE coefficient is only 0.08. The corresponding charts (not shown) for other forecast periods indicate almost identical linear regressions for each of the respective models. Thus, while the (7-L)PE model drastically underforecasts this class of cyclogenesis, Table 1 and Fig. 15 show that it does not perform as badly as the coarser mesh (6-L)PE model. Table 1 shows that only ~10% of the model error is eliminated when the mesh length is halved. Since the diagnostic calculations discussed earlier, based on a continuous model, also

underpredict the deepening rate by about the same amount, it seems unlikely that further improvement in the forecasts can be achieved simply by increasing the horizontal resolution. Important physical ingredients for explosive deepening appear to be missing in the models. The appearance of Fig. 2 suggests that one of the missing ingredients is an adequate representation of the bulk effects of cumulus convection. Additionally, our finding of strong SST gradients being associated with bomb events implies inadequate vertical resolution and planetary-boundary-layer representation in the models.

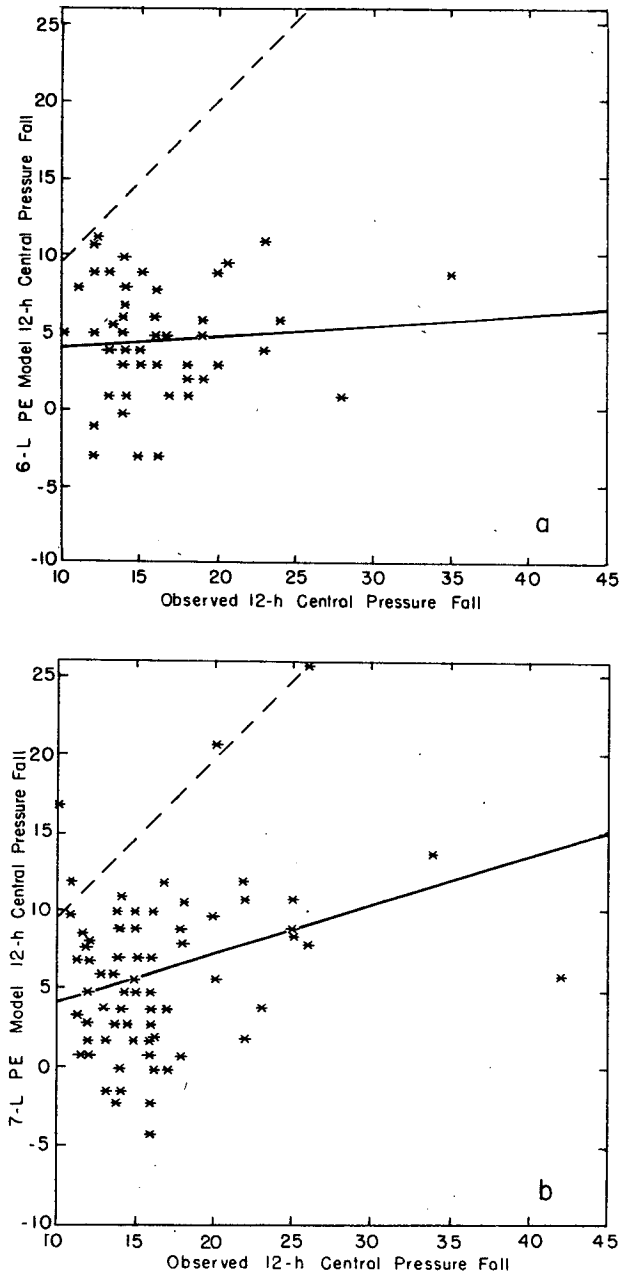

FIG. 15. Plots of observed atmospheric bombs indicating their observed 12 h central pressure fall, and the corresponding PE predicted fall at a forecast range of 12–24 h. Straight line is the least-square regression of the points. Dashed line is the perfect forecast line.

TABLE 2. Summary of atmospheric performance for cases of (7-L)PE predicted bombs. Format is the same as in Table 1.

Forecast period (h)	N	Model 12 h Δp (mb) Mean	Model 12 h Δp (mb) Standard deviation	Observed 12 h Δp (mb) Mean	Observed 12 h Δp (mb) Standard deviation
12–24	9	11.9	2.1	7.1	8.5
24–36	9	11.6	1.1	9.8	7.2
36–48	6	13.3	1.2	9.2	14.1

We have performed an experiment in which a search was conducted for 12 h bombs occurring in the PE atmosphere. The results are presented in Table 2 for the (7-L)PE value during the time period indicated above. The sample size above is quite small, indicating that, though the (7-L)PE is not incapable of simulating explosive storms, it does not do this nearly as often as does the real atmosphere. The (7-L)PE also generally overdevelops these cyclones in comparison with reality. The geographical locations of these 24 PE bombs are indicated in Fig. 16. The individual PE bombs are not mutually exclusive, for three forecast atmospheres are used for the same time period. This one and a half season composite indicates the (7-L)PE develops virtually none of the existing bombs in the Pacific east of the dateline. Most of the (7-L)PE bombs occur in the eastern United States and western Atlantic. A comparison with Fig. 11a indicates the simulation of bombs in the PE atmosphere is displaced well to the south and west of the real atmosphere bombs. The relatively high percentage of continental cases in the PE bomb list and the general overdevelopment of these systems thus appears consistent with Leary's (1971) finding that the (6-L)PE systematically overdevelops some continental cyclones.

8. Conclusions

A rapidly deepening extratropical cyclone has been characterized as one in which the central pressure dropped 1 mb h^{-1} for 24 h. Adopting this rate (suitably adjusted for latitude) as the definition of a meteorological bomb, we have studied the phenomenon during the 3-year period beginning September 1976 in the Northern Hemisphere longitude zone from 120°E eastward to 10°E. We find this explosive cyclogenesis to be a predominately maritime, cold-season event, often with hurricane-like features in the wind and cloud fields.

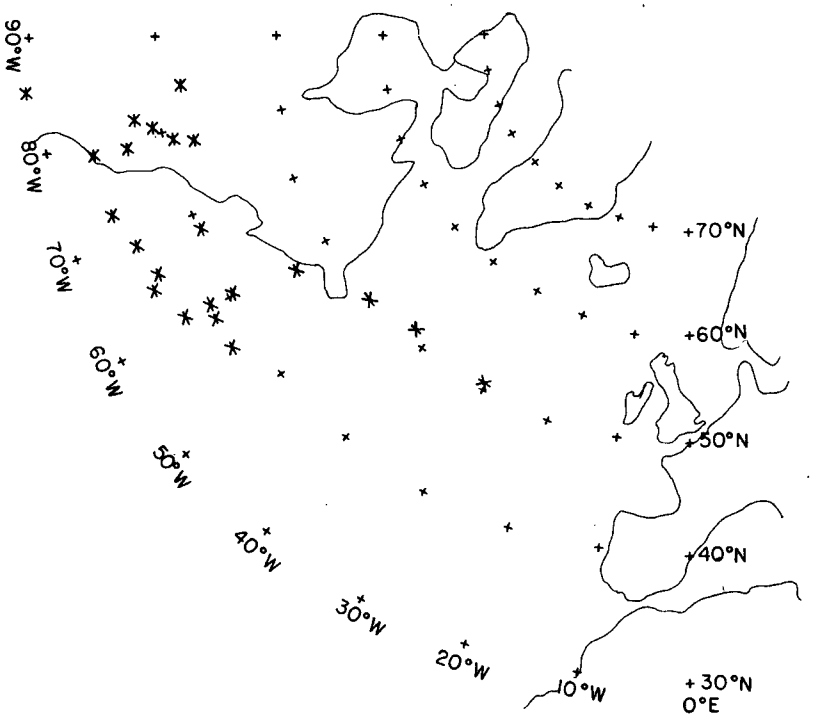

FIG. 16. Locations (indicated by asterisks) of the 22 (7-L)PE bombs at the beginning of their 12 h tracks in the eastern United States and in the Atlantic basin. The two (7-L)PE bombs in the western United States-Pacific domain were located at 42°N, 137°W and at 36°N, 101°W.

The 0000 GMT positions of these surface cyclones were examined in relation to the concurrent positions and configurations of the 552 dam 500 mb contour obtained from the NMC hemispheric analyses. This contour traces out approximately the maximum flow position in middle latitudes. The bomb was generally found 400 n mi downstream from a mobile 500 mb trough, which typically had migrated for several days across the upwind continent before triggering the explosive surface event. The quasi-steady aspects of 500 mb flow, revealed by week-long composites, indicate that bombs almost always occur within or poleward of the main belt of westerlies and within or ahead of the planetary-scale troughs.

We have studied 1978–79 bombs (using a 12 h development criterion) in more detail. This study has shown that explosive cyclogenesis occurs over a wide range of SST's, but, preferentially near the strongest gradients. A composite of surface isobars and tropospheric thicknesses, centered on the incipient bomb, indicates development typically occurs in a region of upper level diffluence. Quasi-geostrophically computed central pressure falls in the composite bomb are far less than the observed falls. Current NMC models also perform poorly in their attempted simulation of observed bombs. However, the models did produce bombs whose geographical pattern indicates a much higher percentage of continental cases than was observed in the real atmosphere. These latter results are consistent with Leary's (1971) study of systematic errors in NMC operational products. We suggest that an adequate representation of the planetary boundary layer and of the bulk effects of cumulus convection is a necessary physical ingredient, missing in the NMC models.

Acknowledgment. The authors are especially grateful to Gene Norman, who contributed substantially to data compilation and composite analysis through the MIT Undergraduate Research Opportunities Program. Gratitude is expressed to the Fleet Numerical Oceanographic Center for providing us with SST analyses. We are indebted to laboratory students Norman Guivens, Tamara Ledley, Giovanna Salustri, Trish Strat, Sandro Rambaldi and George Thurston, for relating surface cyclogenesis to the upper-level flow, and to Isabelle Kole for preparation of manuscript and figures. This research was supported by the Office of Naval Research and by the Naval Environmental Prediction Research Facility under Contract N 00014-79-C-0384.

REFERENCES

Bjerknes, J., 1954: The diffluent upper trough. *Arch. Meteor. Geophys. Bioklim.*, A7, 41–46.

Blackmon, M. L., J. M. Wallace, N-C. Lau and S. L. Mullen,

1977: An observational study of the Northern Hemisphere wintertime circulation. *J. Atmos. Sci.*, **34**, 1040–1053.

Böttger, H., M. Eckardt and U. Katergiannakis, 1975: Forecasting extratropical storms with hurricane intensity using satellite information. *J. Appl. Meteor.*, **14**, 1259–1265.

Dickson, R. R., 1979: Weather and circulation of February 1979-near record cold over northeast quarter of the country. *Mon. Wea. Rev.*, **107**, 624–630.

Druyan, L. M., 1974: Short-range forecasts with the GISS model of the global atmosphere. *Mon. Wea. Rev.*, **102**, 269–279.

Fjørtoft, R., 1952: On a numerical method of integrating the barotropic vorticity equation. *Tellus*, **4**, 179–194.

Frederiksen, J. S., 1979: The effects of long planetary waves on the regions of cyclogenesis: linear theory. *J. Atmos. Sci.*, **36**, 195–204.

Gall, R., R. Blakeslee and R. C. J. Somerville, 1979: Cyclone-scale forcing of ultralong waves. *J. Atmos. Sci.*, **36**, 1692–1698.

Haurwitz, B., and J. M. Austin, 1944: *Climatology* (see p. 187 and Plate XVI). McGraw Hill, 410 pp.

Holliday, C. R., and A. H. Thompson, 1979: Climatological characteristics of rapidly intensifying typhoons. *Mon. Wea. Rev.*, **107**, 1022–1034.

Jalu, M., 1973: Etude des perturbations cycloniques extratropicale par l'imagerie des satellites. *Les Satellites Meteorologiques*, Centre National d'Études Spatiales, 409–422.

Leary, C., 1971: Systematic errors in operational National Meteorological Center primitive-equation surface prognoses. *Mon. Wea. Rev.*, **99**, 409–413.

Miller, B. I., 1958: On the maximum intensity of hurricanes. *J. Meteor.*, **15**, 184–195.

NOAA, 1979: Smooth log, North Atlantic weather, September and October 1978. *Mar. Wea. Log.*, **23**, p. 104.

Petterssen, S., 1956: *Weather Analysis and Forecasting*, Vol. 1, *Motion and Motion Systems*. McGraw-Hill, 428 pp.

Pyke, C. B., 1965: On the role of air-sea interaction in the development of cyclones. *Bull. Amer. Meteor. Soc.*, **46**, 4–15.

Rasmussen, E., 1979: The polar low as an extratropical CISK disturbance. *Quart. J. Roy. Meteor. Soc.*, **105**, 531–549.

Reed, R. J., 1979: Cyclogenesis in polar air streams. *Mon. Wea. Rev.*, **107**, 38–52.

Rice, R. B., 1979: Tracking a killer storm. *Sail*, **10**, 106–107.

Rosenblum, H. S., and F. Sanders, 1974: Meso-analysis of a coastal snow-storm in New England. *Mon. Wea. Rev.*, **102**, 433–442.

Sanders, F., 1971: Analytic solutions of the non-linear omega and vorticity equation for a structurally simple model of disturbances in the baroclinic westerlies. *Mon. Wea. Rev.*, **99**, 393–407.

Shuman, F. G., and J. B. Hovermale, 1968: An operational six-layer primitive equation model. *J. Appl. Meteor.*, **7**, 525–547.

Somerville, R. C. J., P. H. Stone, M. Halson, J. G. Hansen, J. S. Hogan, L. M. Druyan, G. Russell, A. A. Cadis, W. J. Quirk and J. Tenenbaum, 1974: The GISS model of the global atmosphere. *J. Atmos. Sci.*, **31**, 84–117.

Staley, D. O., and R. L. Gall, 1977: On the wavelength of maximum baroclinic instability. *J. Atmos. Sci.*, **34**, 1679–1688.

Sverdrup, H. U., M. W. Johnson and R. H. Fleming, 1942: *The Oceans, Their Physics, Chemistry, and General Biology*. Prentice-Hall, 1087 pp.

Winston, J. S., 1955: Physical aspects of rapid cyclogenesis in the Gulf of Alsaka. *Tellus*, **7**, 481–500.